A Quadrature Sinusoidal Oscillator With Phase-Preserving Wide-Range Linear Frequency Tunability and Frequency-Independent Amplitude

Dimitrios N. Loizos, *Student Member, IEEE*, and Paul P. Sotiriadis, *Member, IEEE*

***Abstract*—A G_m-C architecture for a quadrature sinusoidal oscillator with phase-preserving wide-range linear frequency tunability is discussed. The topology is characterized by low harmonic distortion, as well as controlled and stable amplitude of oscillation that is independent of the oscillation's frequency and instantaneous frequency changes. The architecture has been implemented for acoustic sonar applications using general-purpose discrete bipolar transistors. The phase-preserving frequency control makes the architecture appropriate for continuous-phase frequency-shift keying modulators as well. Measurements and simulation results are presented and found in good agreement with theory.**

***Index Terms*—Amplitude control, continuous-phase frequency-shift keying, frequency control, phase preservation, quadrature oscillator.**

I. Introduction

VARIOUS designs have been proposed for sinusoidal oscillators with tunable oscillation frequency. Most topologies are based on current-controlled current conveyors (CCCII) (e.g., [1]–[4]), operational transconductance amplifiers and capacitors (OTA-Cs) (e.g., [5] and [6]), active resistance–capacitance (RC) networks (e.g., [7]), four-terminal floating nullors (e.g., [8]), and, recently, the translinear principle (e.g., [9] and [10]).

In sinusoidal oscillators, continuous-time wide-range frequency tunability, stable frequency-independent amplitude, and low harmonic distortion are typically antagonistic properties.

In most designs, the amplitude of oscillation is determined by the nonlinearities of the devices and the respective gain saturation, which results in high harmonic distortion [11]. To reduce harmonic distortion, an amplitude feedback control subcircuit can be added (e.g., [7] and [12]) to keep the oscillation amplitude to appropriate levels, so that the nonlinearities of the devices are not excited. However, designing the feedback loop is not trivial. As shown in [12] and [13], dynamic amplitude feedback control can easily result in instabilities. Instabilities are interpreted as continuous fluctuation of the oscillation's amplitude, and the amount of fluctuation may depend on the initial condition of the feedback loop.

Several schemes for amplitude control have been proposed. In [14], the original and an improved version of Van der Pol's model, which effectively decouples frequency and amplitude control, are discussed. An extended analysis of the tradeoff between settling time and distortion in Van der Pol's model is given in [15]. In [16], a quadrature oscillator is proposed where the square of the oscillation's amplitude is fed back to a variable resistance. A similar approach but with signals of 135° phase difference has been suggested in [7]. The dynamic feedback loop used in [7], however, is subject to stability issues during transitions from one frequency or amplitude level to another. In [12], a more careful design of the control system has been presented where the feedback system controls both the quality factor Q and the amplitude of the oscillator, achieving a stable amplitude of oscillation; yet, the oscillation is narrow frequency band. In [17], a static amplitude control configuration has been proposed using operational amplifiers and multipliers.

The wide-tuning-range quadrature oscillator architecture proposed in this brief resolves the amplitude problem using a static (nondynamic) amplitude feedback loop and translinear circuits. The architecture achieves independence between frequency and amplitude control, instantaneous frequency control, low harmonic distortion, and stable oscillation amplitude. Moreover, the frequency control is phase preserving, making this architecture ideal for use in continuous-phase frequency-shift keying (FSK) modulators. The validity of the proposed architecture was demonstrated by detailed simulation, as well as by building the oscillator with discrete general-purpose components. Measurements and simulation results are presented and found to be in good agreement with theory.

II. Theoretical Analysis

A state-space representation of an ideal (i.e., lossless) second-order G_m-C quadrature oscillator (Fig. 1) is of the form

$$\dot{V}_1(t) = \frac{G_m(t)}{C}V_2(t)$$
$$\dot{V}_2(t) = -\frac{G_m(t)}{C}V_1(t) \tag{1}$$

where $V_1(t)$ and $V_2(t)$ are the voltages on the capacitors and state variables of the system. System (1) is lossless. The oscillation has a constant amplitude, which depends on the initial conditions, and (instantaneous) frequency,[1] given by

$$\omega(t) = 2\pi f(t) = \dot{\theta}(t) = \frac{G_m(t)}{C}. \tag{2}$$

The advantage of system (1) is that frequency $\omega(t)$ is instantaneously controlled by the value of the transconductance $G_m(t)$

Manuscript received May 31, 2005; revised March 20, 2006. This paper was recommended by Associate Editor J. Liu.

The authors are with the Department of Electrical and Computer Engineering, The Johns Hopkins University, Baltimore, MD 21218 USA (e-mail: dloizos@jhu.edu; pps@jhu.edu).

Digital Object Identifier 10.1109/TCSII.2006.882359

[1]The solution of (1) is $V_1(t) = A_0\sin(\theta(t))$ and $V_2(t) = A_0\cos(\theta(t))$, where $\theta(t) = \int_0^t \omega(\tau)d\tau + \theta_0$ and $\omega(t) = G_m(t)/C$. A_0 depends on the initial conditions and is equal to $A_0 = \sqrt{V_1^2(0) + V_2^2(0)}$.

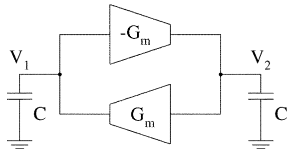

Fig. 1. Ideal second-order $G_m - C$ oscillator.

as indicated by expression (2). This property of the oscillator is desirable in several applications.

However, the amplitude of the oscillation is not controlled by any voltage or current; it depends only on the initial conditions $V_1(0)$ and $V_2(0)$. Furthermore, any circuit implementation of system (1) will exhibit some additional parasitic dynamic that will either damp or overamplify the oscillation, saturate the transconductors, and introduce high harmonic distortion.

To control the oscillation amplitude while maintaining the instantaneous frequency control and phase continuity, we modify system (1) as

$$\dot{V}_1(t) = \frac{G_m(t)}{C} V_2(t) + K(\mathbf{V}(t)) V_1(t)$$
$$\dot{V}_2(t) = -\frac{G_m(t)}{C} V_1(t) + K(\mathbf{V}(t)) V_2(t). \qquad (3)$$

Again, the state vector is $\mathbf{V}(t) = [V_1(t), V_2(t)]^T$. The scalar function $K(\cdot)$ is appropriately chosen to force the oscillation amplitude to a desirable value while allowing the phase and amplitude to evolve and be controlled independently. Note that since $K(\cdot)$ is a scalar function, no dynamics are added to system (1), and therefore, the amplitude control is static.

Consider the transformation of the state variables into polar coordinates $V_1(t) = A(t)\sin\theta(t)$ and $V_2(t) = A(t)\cos\theta(t)$, where $A(t) = \sqrt{V_1^2(t) + V_2^2(t)} = \|\mathbf{V}(t)\|$ is the instantaneous amplitude and $\theta(t) = \angle(V_1(t), V_2(t))$ is the instantaneous phase. System (3) in polar coordinates and matrix notation is written as

$$\begin{bmatrix} \cos\theta(t) & \sin\theta(t) \\ -\sin\theta(t) & \cos\theta(t) \end{bmatrix} \begin{bmatrix} \dot{\theta}(t) \\ \dot{A}(t)/A(t) \end{bmatrix} = \begin{bmatrix} \cos\theta(t) & \sin\theta(t) \\ -\sin\theta(t) & \cos\theta(t) \end{bmatrix} \begin{bmatrix} \frac{G_m(t)}{C} \\ K(\mathbf{V}(t)) \end{bmatrix}. \qquad (4)$$

Since both sides of (4) are left multiplications by a unitary, and thus invertible, matrix, we conclude that

$$\dot{\theta}(t) = \frac{G_m(t)}{C} \qquad (5)$$
$$\dot{A}(t) = K(\mathbf{V}(t)) A(t). \qquad (6)$$

Although (5) shows that the frequency is instantaneously controlled by $G_m(t)$ and is independent of the amplitude, the amplitude $A(t)$ may depend on the phase $\theta(t)$ through the voltage vector $\mathbf{V}$. However, if function K is of the special form $K(\mathbf{V}) = k(A)$, then differential equation (6) becomes

$$\dot{A}(t) = k(A(t)) A(t) \qquad (7)$$

implying that the amplitude is independent of the phase and the frequency. The choice of function $k(\cdot)$ is important since it dictates whether the amplitude reaches a desirable steady-state value A_{ref} and, if so, how fast it converges. For example, if k is such that $k(A) > 0$ when $A < A_{\text{ref}}$ and $k(A) < 0$ when $A > A_{\text{ref}}$, then given that $A > 0$, it is $\lim_{t\to\infty} A(t) = A_{\text{ref}}$ for every nonzero initial vector $\mathbf{V}(0)$.

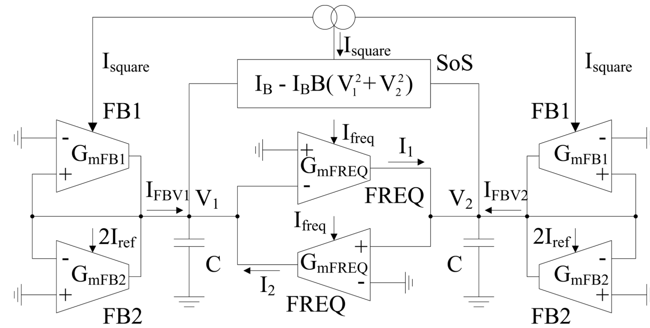

Fig. 2. Block diagram of the architecture.

Equation (7) can be solved analytically for several convenient choices of k. To simplify the circuit implementation of the architecture, function k was chosen as $k(A) = G(A_{\text{ref}}^2 - A^2)$, where G is a gain factor as well. Solving (7), for nonzero initial conditions, we have

$$A(t) = \frac{A_{\text{ref}}}{\sqrt{1 - \left(1 - \left(\frac{A_{\text{ref}}}{A(0)}\right)^2\right) e^{-2GA_{\text{ref}}^2 t}}}. \qquad (8)$$

From (8), $\lim_{t\to\infty} A(t) = A_{\text{ref}}$ and $A(t)$ approaches A_{ref} exponentially fast in a neighborhood of A_{ref} since

$$A(t) = A_{\text{ref}} \left[1 + \left(1 - \frac{A_{\text{ref}}^2}{A(0)^2}\right) e^{-2GA_{\text{ref}}^2 t}\right] + O\left(e^{-4GA_{\text{ref}}^2 t}\right).$$

In the general case, function $k(\cdot)$ can be chosen as $k(A) = f(A_{\text{ref}}) - f(A)$, where f is a strictly increasing function. A_{ref} would then be an asymptotically stable equilibrium point of (7) and steady state would be reached when $k(A) = 0$.

III. Architecture and Circuit of the Oscillator

The architecture shown in Fig. 2 has been implemented according to the theoretical analysis of Section II. Current I_{freq} controls transconductance G_{mFREQ} and, through (2), the frequency of oscillation. The amplitude is controlled by the remaining blocks that form a static (nondynamic) feedback loop. More specifically, the "sum of squares" (SoS) block generates current $I_{\text{square}} = I_B B(B^{-1} - \|\mathbf{V}\|^2) = I_B B(B^{-1} - A^2)$ that controls the transconductance G_{mFB1} of the FB1 transconductors and whose form is very close to the control function we want to implement. However, since B is a constant, an extra term is required to achieve controllability of the amplitude of oscillation. This term is provided by the FB2 transconductors, whose transconductance G_{mFB2} is controlled by the current $2I_{\text{ref}}$.

A. Transconductor Design

The transconductor is shown in Fig. 3(a). To achieve high linearity, the *Caprio* quad [18] was used [transistors Q_1–Q_4 and resistor R in Fig. 3(a)].

The gain of the transconductor is linearly controlled by the tail current I_{freq} of the differential pair Q_{y1} and Q_{y2}. Transistors Q_{x1}, Q_{y1}, Q_{y2}, and Q_{x2}, in Fig. 3(a) form a gain controllable differential current mirror, known as the *Gilbert* gain cell [19].

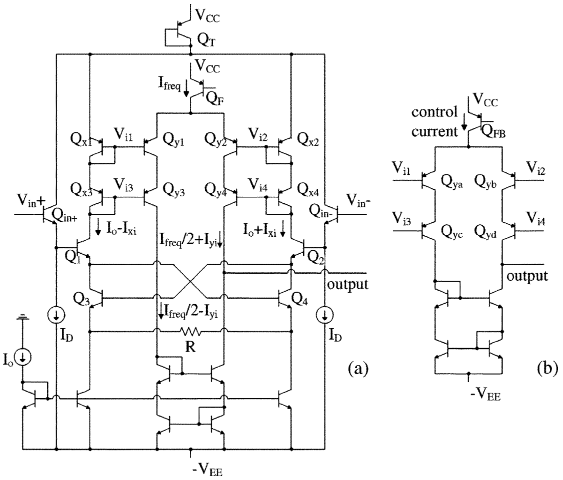

Fig. 3. Circuits of (a) the complete and (b) the reduced transconductors.

Transistor Q_T is used for biasing correctly transistors Q_{y1} to Q_{y4}. The total gain of the transconductor is (output current over the differential input voltage $V_{\rm in}^+ - V_{\rm in}^-$)

$$G_{\rm mFREQ} = \frac{I_{\rm freq}}{I_o R}. \tag{9}$$

The emitter followers $Q_{\rm in+}$ and $Q_{\rm in-}$ are used to increase the input impedance of the transconductor. High output impedance is achieved using the cascode configuration at the output stage.

B. "Reduced" Transconductors

Although the architecture of Fig. 2 requires six transconductors, all of them share only two inputs, i.e., V_1 and V_2. Thus, there is no need to replicate the entire circuit of Fig. 3(a) six times.

Instead, we use it to implement only the two frequency (FREQ) transconductors (Fig. 2). The output currents of the other transconductors are generated by the reduced circuit(s) of Fig. 3(b), whose inputs, i.e., V_{i1} to V_{i4}, are connected to the bases of transistors Q_{x1} to Q_{x4} of the FREQ transconductors [Fig. 3(a)]. This way, the total number of transistors decreases dramatically without significantly degrading the performance of the oscillator.

The control (tail) current in Fig. 3(b) is equal to $I_{\rm square}$ for transconductors FB1 and $2I_{\rm ref}$ for transconductors FB2. Using the translinear principle [18], it can be directly verified from Fig. 3 that

$$G_{\rm mFB1} = \frac{I_{\rm square}}{I_o R} \text{ and } G_{\rm mFB2} = \frac{2I_{\rm ref}}{I_o R}. \tag{10}$$

C. Generation of $I_{\rm square}$

The circuit block of Fig. 4 generates the amplitude control current $I_{\rm square} = I_B B(B^{-1} - A^2)$. It operates in current mode and uses Gilbert's gain cell [19]. Again, to reduce the overall circuit complexity, the input parts of the FREQ transconductors are reused to drive the translinear circuit of Fig. 4; its inputs V_{i1} and V_{i2}, $i = 1, 2$, are connected to the bases of Q_{x1} and Q_{x2}.

To derive the exact function implemented by the SoS block, we start by applying the translinear principle to the loop formed by transistors Q_{1A} to Q_{1D} (Q_{2A} to Q_{2D}, respectively), which gives $I_{si} = (I_B^2 - I_{fi}^2)/(2I_B)$, $i = 1, 2$. Since $I_{\rm square} = I_{s1} + I_{s2}$, we get

$$I_{\rm square} = I_B - \frac{I_{f1}^2 + I_{f2}^2}{2I_B}. \tag{11}$$

The gain cells formed by transistors Q_{x1} and Q_{x2} in Fig. 3(a) and Q_{Fi1} and Q_{Fi2} in Fig. 4 relate currents I_{fi} to currents I_{xi} through $I_{fi} = I_B I_{xi}/I_o$, $i = 1, 2$.

Using the relations $I_{xi} = V_i/R$, $i = 1, 2$, resulting from the *Caprio* quads [18] in the FREQ transconductors, we conclude that $I_{fi} = I_B V_i/(R I_o)$, $i = 1, 2$. Finally, replacing the last equations into (11), we get

$$I_{\rm square} = I_B \left(1 - \frac{V_1^2 + V_2^2}{2I_o^2 R^2}\right). \tag{12}$$

Current $I_{\rm square}$ is mirrored as the control current of the feedback transconductors FB1 (Fig. 2).

D. Operation and Limitations

The oscillation frequency is defined by the capacitors' value and the gain $G_{\rm mFREQ}$ of the FREQ transconductors. From (5) and (9), we conclude that

$$f = \frac{G_{\rm mFREQ}}{2\pi C} = \frac{I_{\rm freq}}{2\pi I_o R C}. \tag{13}$$

This demonstrates a linear relationship between the frequency of oscillation and the frequency control current $I_{\rm freq}$.

The amplitude of oscillation is determined by the amplitude feedback loop in Fig. 2. Specifically, the terms $K(\mathbf{V}(t))V_i(t)$, $i = 1, 2$, in (3) are realized by $I_{{\rm FBV}i}/C$ in Fig. 2. Since $I_{{\rm FBV}i} = (G_{\rm mFB1} - G_{\rm mFB2})V_i$, using (10), we get that

$$I_{{\rm FBV}i} = \frac{I_{\rm square} - 2I_{\rm ref}}{I_o R} \cdot V_i, \qquad i = 1, 2. \tag{14}$$

Replacing (12) in (14), we conclude that the total currents provided to the capacitors by the amplitude feedback loop are

$$I_{{\rm FBV}i} = \frac{I_B}{I_o R}\left(1 - \frac{2I_{\rm ref}}{I_B} - \frac{V_1^2 + V_2^2}{2I_o^2 R^2}\right) V_i, \qquad i = 1, 2. \tag{15}$$

Since $I_{{\rm FBV}i} = CK(\mathbf{V}(t))V_i$, we have that

$$K(\mathbf{V}(t)) = \frac{I_B}{I_o R C}\left(1 - \frac{2I_{\rm ref}}{I_B} - \frac{V_1^2 + V_2^2}{2I_o^2 R^2}\right). \tag{16}$$

The oscillation amplitude is derived setting $K(\mathbf{V}(t)) = 0$, i.e.,

$$A_{\rm ref} = \sqrt{2} I_o R \sqrt{1 - \frac{2I_{\rm ref}}{I_B}}. \tag{17}$$

From (17), we see that $I_{\rm ref}$ must be less than half of I_B. Moreover, the current V_i/R flowing through each resistor R in the *Caprio* quads [Fig. 3(a)] cannot be larger than the biasing current I_o of the transconductors (note also that $|V_i| \le A_{\rm ref}$). Combining these two constraints, we get the bounding conditions for $I_{\rm ref}$, i.e., $0.25 I_B \le I_{\rm ref} \le 0.5 I_B$.

The finite input and output impedances of the transconductors can be jointly modeled as a parasitic resistance $R_{\rm par}$ in parallel with the capacitors C (Fig. 2). The effect of this parasitic

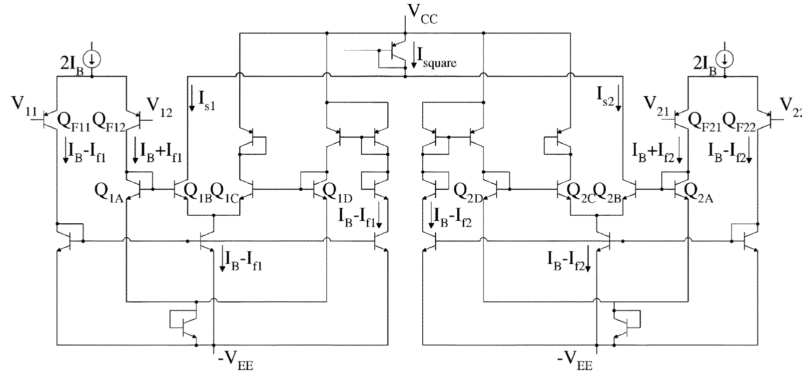

Fig. 4. Translinear circuit implementation of the SoS function.

resistance can be incorporated into (15) as an additional term $V_i/R_{\rm par}$. Accounting for this term, (17) takes the form

$$A_{\rm ref} = \sqrt{2} I_o R \sqrt{1 - \frac{2I_{\rm ref}}{I_B} + \frac{I_o R}{I_B R_{\rm par}}}. \tag{18}$$

Considering the parasitic resistance $R_{\rm par}$ in the model of the proposed architecture does not affect the attribute of independence between the instantaneous frequency and amplitude control demonstrated by (5) since the effect of $R_{\rm par}$ can be incorporated in function $K(\mathbf{V}(t))$.

However, $R_{\rm par}$ affects the attribute of independence between the amplitude and frequency controls. The output resistance of the $G_{\rm mFREQ}$ transconductors depends on current $I_{\rm freq}$ and, therefore, so does $R_{\rm par}$. As can be seen from (18), if all biasing control currents are kept constant except for $I_{\rm freq}$, $A_{\rm ref}$ will change. The variation in $A_{\rm ref}$ due to $I_{\rm freq}$ depends on biasing currents I_o, I_B, and $I_{\rm freq}$ and resistance R.

IV. Measurements and Simulation Results

The circuit blocks described in Section III were used to implement the oscillator's architecture of Fig. 2. The circuit was built using the general-purpose n-p-n and p-n-p discrete bipolar transistors 2N3390 and 2N3702, respectively ($f_T \sim 100$ MHz), 8 ± 0.5 nF capacitors and 1 ± 0.05 kΩ resistors.

The biasing current I_o of the FREQ transconductors [Fig. 3(a)] was set to 360 μA, whereas current I_B in the SoS block was set to 1 mA. For the biasing current I_D of the emitter followers $Q_{\rm in+}$ and $Q_{\rm in-}$ of the FREQ transconductors [Fig. 3(a)], a value of 10 μA was chosen. The power supply was set to $V_{\rm CC} = 3$ V and $V_{\rm EE} = -3$ V. The power dissipation is a function of both frequency and amplitude of oscillation. For a frequency of 10 kHz and amplitude of 250 mV, the power consumption was found approximately equal to 80 mW. Also, for the same case, the time constant $(2GA_{\rm ref}^2)^{-1}$ in equation (8), which describes how fast the amplitude converges to the steady state, was approximately 2 μs.

The linear relation between the oscillation frequency and current $I_{\rm freq}$ is shown in Fig. 5. Both measurements and simulation are in very close agreement with theory.

In Fig. 6, current $I_{\rm freq}$ is generated by an external waveform generator (channel 2). As shown in the graph, the frequency of oscillation changes instantaneously, whereas the amplitude remains constant. In addition, the instantaneous phase does not change when the frequency changes at the rise or fall of the frequency control current pulse.

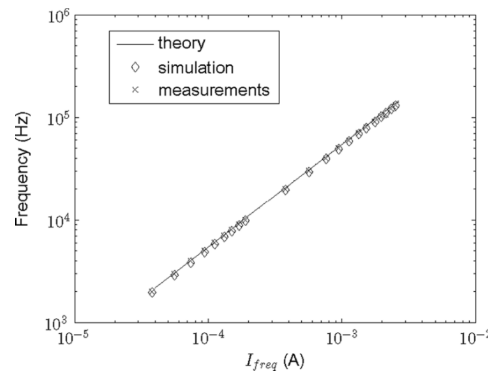

Fig. 5. Oscillation frequency versus $I_{\rm freq}$.

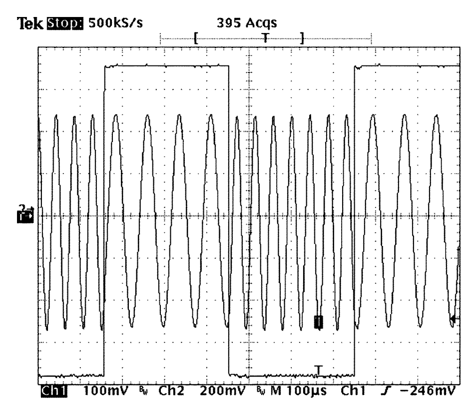

Fig. 6. Snapshot showing the instantaneous control of frequency and the independence of the amplitude.

Fig. 7 shows how voltages V_1 and V_2 evolve in time. Using fast Fourier transformation (FFT) in both simulation and experimental results, it was possible to find the phase difference between the two state variables V_1 and V_2. This phase difference was measured to be $90^\circ \pm 0.5^\circ$ for all frequencies in the range from 7 to 80 kHz, demonstrating the quadrature behavior of the oscillator.

Measurements shown in Fig. 8 demonstrate low total harmonic distortion for frequencies ranging from 7 to 80 kHz. The data were recorded keeping $I_{\rm ref}$ constant at 306 μA and sweeping $I_{\rm freq}$. On the same figure, simulation results showing how the amplitude of oscillation varies with frequency while keeping $I_{\rm ref}$ constant are also demonstrated. In the range of 7–80 kHz, the variation in amplitude is less than approximately

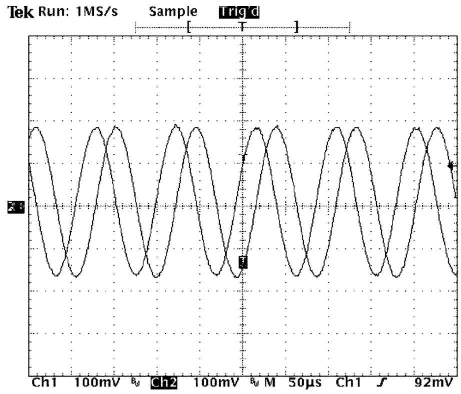

Fig. 7. Snapshot showing $V_1(t)$, $V_2(t)$, and their 90° phase difference.

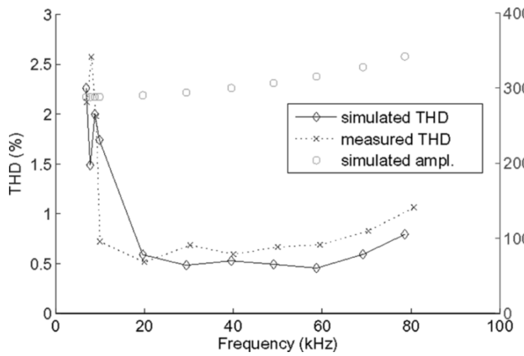

Fig. 8. Measured and simulated total harmonic distortion for $I_{\mathrm{ref}} = 306\ \mu$A. Variation of the amplitude is also shown as frequency increases.

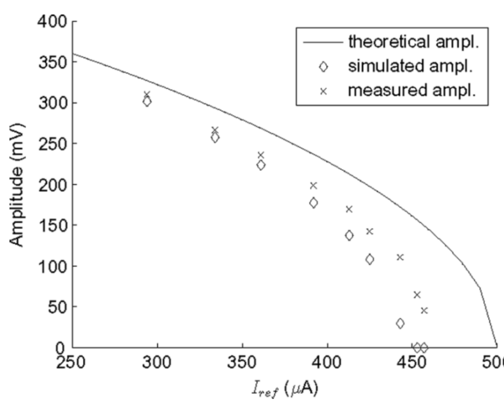

Fig. 9. Relation between the amplitude of oscillation and I_{ref}. I_{freq} has been kept constant at 184 μA.

10%. This variation can be further reduced if devices with higher output resistance are used.

It should be noted that oscillations with distortion less than 2% can be observed for frequencies up to 130 kHz. However, for frequencies higher than 80 kHz, I_{ref} needs to be tweaked appropriately so as to keep the amplitude of oscillation constant. For the maximum attained frequency (130 kHz) and for a total amplitude of the V_1 and V_2 signals set to 243 mV, the fundamental harmonic had an amplitude of 240 mV, the second of 300 μV, and the third of 386 μV.

Simulation and measurements were also conducted for the case where current I_{freq} controlling the frequency of oscillation was kept constant, whereas current I_{ref} was swept between the limits specified in Section III. The results are shown in Fig. 9 and demonstrate good agreement between theory (17), simulation, and experiment.

Finally, the topology was also simulated using RF bipolar junction transistors (BJTs) of high f_T, namely the Philips BFG540 n-p-n and the Philips BFT92 p-n-p. The only alteration to the circuit was changing the capacitors to 50 pF. Simulation showed that oscillations up to 6.5 MHz were generated with very low harmonic distortion.

V. Conclusion

A $G_m - C$ architecture for quadrature sinusoidal oscillators using a static amplitude control feedback loop has been analyzed and implemented. It is characterized by linear frequency control, phase preservation during frequency hoping, and constant amplitude that is frequency and phase independent. The implemented oscillator has wide-range frequency tunability and low harmonic distortion. The theoretical results were verified by measurements and simulation.

References

[1] W. Kiranon, J. Kesorn, and P. Wardkein, "Current controlled oscillator based on translinear conveyors," *Electron. Lett.*, vol. 32, no. 15, pp. 1330–1331, Jul. 1996.

[2] H. Barthelemy, S. Meillere, and E. Kussener, "CMOS sinusoidal oscillator based on current-controlled current conveyors," *Electron. Lett.*, vol. 38, no. 21, pp. 1254–1256, Oct. 2002.

[3] A. Fabre, O. Saaid, F. West, and C. Boucheron, "High frequency applications based on a new current controlled conveyor," *IEEE Trans. Circuits Syst.*, vol. 43, no. 2, pp. 82–91, Feb. 1996.

[4] M. T. Abuelma'atti and M. A. Al-Qahtani, "A new current-controlled multiphase sinusoidal oscillator using translinear current conveyors," *IEEE Trans. Circuits Syst. II, Analog Digit. Signal Process.*, vol. 45, no. 7, pp. 881–885, Jul. 1998.

[5] J. Galan, R. G. Carvajal, A. Torralba, F. Munoz, and J. Ramirez-Angulo, "A low-power low-voltage OTA-C sinusoidal oscillator with a large tuning range," *IEEE Trans. Circuits Syst. I, Reg. Papers*, vol. 52, no. 2, pp. 283–291, Feb. 2005.

[6] J. A. De Lima, "A linearly-tunable OTA-C sinusoidal oscillator for low-voltage applications," in *Proc. ISCAS*, May 26–29, 2002, vol. 2, pp. 408–411.

[7] J. I. Osa and A. Carlosena, "MOSFET-C sinusoidal oscillator with variable frequency and amplitude," in *Proc. ISCAS*, May 28–31, 2000, vol. 2, pp. 725–728.

[8] M. T. Abuelma'atti and H. A. Al-Zaher, "Current-mode sinusoidal oscillators using single FTFN," *IEEE Trans. Circuits Syst. II, Analog Digit. Signal Process.*, vol. 46, no. 1, pp. 69–74, Jan. 1999.

[9] W. A. Serdijn, J. Mulder, A. C. van der Woerd, and A. H. M. van Roermund, "A wide-tunable translinear second-order oscillator," *IEEE J. Solid-State Circuits*, vol. 33, no. 2, pp. 195–201, Feb. 1998.

[10] N. Fragoulis and I. Haritantis, "A low-voltage quadrature log-domain oscillator," in *Proc. 9th Int. Conf. Electron., Circuits Syst.*, 2002, vol. 1, pp. 101–104.

[11] D. Pederson and K. Mayaram, *Analog Integrated Circuits for Communication : Principles, Simulation and Design*. New York: Springer-Verlag, 1990.

[12] D. Li and Y. Tsividis, "A loss-control feedback loop for VCO indirect tuning of RF integrated filters," *IEEE Trans. Circuits Syst.*, vol. 47, no. 3, pp. 169–175, Mar. 2000.

[13] T. H. O'Dell, "Instability of an oscillator amplitude control system," *Proc. Inst. Electr. Eng.—Control Theory and Applications*, vol. 151, no. 2, pp. 194–197, Mar. 2004.

[14] B. Z. Kaplan and I. Yaffe, "An improved van der Pol equation and some of its possible applications," *Int. J. Electron.*, vol. 41, no. 2, pp. 189–198, 1976.

[15] W. B. Mikhael and S. Tu, "Continuous and switched-capacitor multiphase oscillators," *IEEE Trans. Circuits Syst.*, vol. CAS-31, no. 3, pp. 280–293, Mar. 1984.

[16] I. M. Filanovsky and L. F. Taylor, "A comparison of two models for an oscillator with an amplitude control system," *IEEE Trans. Circuits Syst.*, vol. CAS-34, no. 9, pp. 1110–1112, Sep. 1987.

[17] I. M. Filanovsky, "Sinusoidal VCO with control of frequency and amplitude," in *Proc. 32nd Midwest Symp. Circuits and Syst.*, Champaign, IL, Aug. 14–16, 1989, vol. 1, pp. 446–449.

[18] C. Toumazou, F. J. Lidgey, and D. G. Haigh, *Analogue IC Design: The Current-Mode Approach*. London, U.K.: Peter Peregrinus, 1990.

[19] B. Gilbert, "A new wideband amplifier technique," *IEEE J. Solid-State Circuits*, vol. SC-3, no. 4, pp. 353–365, Dec. 1968.